Journal of Autoimmunity 108 (2020) 102379

Contents lists available at ScienceDirect

Journal of Autoimmunity

journal homepage: www.elsevier.com/locate/jautimm

Histone deacetylase 1 (HDAC1): A key player of T cell-mediated arthritis

Lisa Göschl[a], Teresa Preglej[b], Nicole Boucheron[b], Victoria Saferding[a,n], Lena Müller[a,n], Alexander Platzer[a], Kiyoshi Hirahara[c,d], Han-Yu Shih[e], Johan Backlund[f], Patrick Matthias[g,h], Birgit Niederreiter[a], Anastasiya Hladik[i,j], Maximilian Kugler[a], Guido A. Gualdoni[b,k], Clemens Scheinecker[a], Sylvia Knapp[i,j], Christian Seiser[l], Rikard Holmdahl[f], Katharina Tillmann[m], Roberto Plasenzotti[m], Bruno Podesser[m], Daniel Aletaha[a], Josef S. Smolen[a], Thomas Karonitsch[a], Günter Steiner[a,n], Wilfried Ellmeier[b], Michael Bonelli[a,*]

[a] Division of Rheumatology, Department of Internal Medicine III, Medical University of Vienna, 1090, Vienna, Austria
[b] Division of Immunobiology, Institute of Immunology, Center for Pathophysiology, Infectiology and Immunology, Medical University of Vienna, 1090, Vienna, Austria
[c] Department of Immunology, Graduate School of Medicine, Chiba University, Chiba, 260-8670, Japan
[d] AMED-PRIME, AMED, Chiba, 260-8670, Japan
[e] Molecular Immunology and Inflammation Branch, National Institute of Arthritis, Musculoskeletal and Skin Diseases, National Institutes of Health, Bethesda, United States
[f] Department of Medical Biochemistry and Biophysics, Medical Inflammation Research, Karolinska Institute, 17177, Stockholm, Sweden
[g] Friedrich Miescher Institute for Biomedical Research, 4058, Basel, Switzerland
[h] Faculty of Sciences, University of Basel, 4031, Basel, Switzerland
[i] Research Center for Molecular Medicine of the Austrian Academy of Sciences (CeMM), Vienna, Austria
[j] Laboratory of Infection Biology, Department of Internal Medicine I, Medical University of Vienna, 1090, Vienna, Austria
[k] Division of Nephrology and Dialysis, Department of Internal Medicine III, Medical University of Vienna, 1090, Vienna, Austria
[l] Division of Cell and Developmental Biology, Center for Anatomy and Cell Biology, Medical University of Vienna, Vienna, Austria
[m] Division of Biomedical Research, Medical University of Vienna, 1090, Vienna, Austria
[n] Ludwig Boltzmann Institute for Arthritis and Rehabilitation, 1090, Vienna, Austria

ARTICLE INFO

Keywords:
Histone deacetylases
HDACs
Rheumatoid arthritis
T cells
CCR6

ABSTRACT

Rheumatoid Arthritis (RA) represents a chronic T cell-mediated inflammatory autoimmune disease. Studies have shown that epigenetic mechanisms contribute to the pathogenesis of RA. Histone deacetylases (HDACs) represent one important group of epigenetic regulators. However, the role of individual HDAC members for the pathogenesis of arthritis is still unknown. In this study we demonstrate that mice with a T cell-specific deletion of HDAC1 (*HDAC1-cKO*) are resistant to the development of Collagen-induced arthritis (CIA), whereas the antibody response to collagen type II was undisturbed, indicating an unaltered T cell-mediated B cell activation. The inflammatory cytokines IL-17 and IL-6 were significantly decreased in sera of *HDAC1-cKO* mice. IL-6 treated HDAC1-deficient $CD4^+$ T cells showed an impaired upregulation of CCR6. Selective inhibition of class I HDACs with the HDAC inhibitor MS-275 under Th17-skewing conditions inhibited the upregulation of chemokine receptor 6 (CCR6) in mouse and human $CD4^+$ T cells. Accordingly, analysis of human RNA-sequencing (RNA-seq) data and histological analysis of synovial tissue samples from human RA patients revealed the existence of $CD4^+CCR6^+$ cells with enhanced HDAC1 expression. Our data indicate a key role for HDAC1 for the pathogenesis of CIA and suggest that HDAC1 and other class I HDACs might be promising targets of selective HDAC inhibitors (HDACi) for the treatment of RA.

1. Introduction

Rheumatoid Arthritis (RA) is a chronic inflammatory autoimmune disease, which leads to irreversible destruction of the joints. Despite big efforts to develop new therapeutic strategies there is still a large number of patients who fail to respond to current therapies [1]. The

Abbreviations: CCR, chemokine receptor; CFA, complete Freund's adjuvant; CIA, collagen induced arthritis; CII, collagen type II; FLS, fibroblast-like synoviocytes; HDAC, histone deacetylase; HDACi, HDAC inhibitor; KLH, keyhole limpet hemocyanin; RA, rheumatoid arthritis; RNA-seq, RNA sequencing; STAT, signal transducer and activator of transcription; TF, transcription factors; Th, T helper

* Corresponding author.
E-mail address: michael.bonelli@meduniwien.ac.at (M. Bonelli).

https://doi.org/10.1016/j.jaut.2019.102379
Received 25 June 2019; Received in revised form 20 September 2019; Accepted 2 December 2019
Available online 26 December 2019

interplay of various immune cells leads to local and systemic inflammation. T cells play a central role in the pathogenesis of RA due to their capacity to drive activation of B cells, monocytes, macrophages and fibroblast-like synoviocytes (FLS) [2]. T cells occur in high numbers in synovial infiltrates and are considered major culprits in arthritis development. Various $CD4^+$ T cell subsets and their lineage-specific cytokines contribute to the inflammatory cascade. $CD4^+$ T cell lineage identity is determined by the expression of specific master transcription factors (TF) [3]. Binding of TF is regulated by epigenetic modifications, such as posttranslational histone modifications. Recruitment of TF and co-factors to specific enhancer regions can thereby ensure a specific lineage identity.

One of the best-characterized histone modifications is the reversible acetylation of lysine residues, which is regulated by the opposing enzyme families of histone acetyltransferases (HATs) and histone deacetylases (HDACs). HDACs modify epigenetic landscapes by removing acetyl groups of lysine residues of histones, which results in chromatin condensation and repression of transcription [4]. In mammals, 18 members of the HDAC family have been identified and are divided into four subclasses according to their homology to yeast enzymes [4–7]. Various HDAC members are also key regulators of T cell subset differentiation and T cell-mediated autoimmune diseases [5]. In case of RA, a dysregulation of HDACs in peripheral blood mononuclear cells (PBMCs), macrophages and FLS were associated with a higher disease activity [6–10]. In line with this, HDACi exhibit a potential as anti-inflammatory drugs in various murine arthritis models [11–17]. We previously showed that HDAC1 activity in $CD4^+$ T cells is crucial for the development of experimental autoimmune encephalitis (EAE) [18]. However, whether HDAC1 in $CD4^+$ T cells is a key player for the development of arthritis has not been investigated. In this study we show that a conditional deletion of HDAC1 in the T cell lineage leads to a complete protection of CIA, a murine model which resembles rheumatoid arthritis. Reduced serum levels of IL-6 and IL-17 where detected during different phases of the disease, revealing a potential role of HDAC1 in the production of pro-inflammatory cytokines. Upregulation of the chemokine receptor CCR6, which is important for the induction of CIA [1,19], was impaired in IL-6 cultured HDAC1-deficient $CD4^+$ T cells as well as murine and human Th17 cells treated with selective class I HDACi. Taken together, our data reveal HDAC1 and class I HDACs as a potential new target for the treatment of RA.

2. Methods

2.1. Animal models

All experiments were approved by the local ethics committee. Animal experiments were evaluated by the ethics committee of the Medical University of Vienna and approved by the Federal Ministry for Science and Research, Vienna, Austria (GZ: BMWF-66.009/0347-WF/V/3b/2016). $Hdac1^{flox/flox}$ were crossed to the $Cd4^{Cre}$ mice as previously described [18,20]. Animal husbandry and experimentation was performed under national laws (Federal Ministry for Science and Research, Vienna, Austria) and according to the guidelines of FELASA which match that of ARRIVE. All mice were analyzed 8–18 weeks of age and of mixed sex unless otherwise stated. Littermate controls were used for all experiments.

2.2. Induction of CIA

HDAC1-cKO mice and littermate controls were immunized subcutaneously with 50 μg chicken type II collagen (Sigma-Aldrich) in 50 μl H2O, emulsified in 50 μl Freund's complete adjuvant, enriched with 10 μg/ml *Mycobacterium tuberculosis* (H37Ra; Difco/BD Biosciences), on day 1 and day 21, as previously described [21]. Mice in this disease model are expected to develop arthritis between week 3 and week 10 and were evaluated twice a week for symptoms of arthritis using a semi-quantitative scoring system including the degree of joint swelling and grip strength. Briefly, joint swelling was examined using a clinical score ranging from 0 to 3 (0 no swelling, 1 mild swelling of the toes and ankle, 2 moderate swelling of the toes and ankle, and 3 severe swelling of the toes and ankle). In addition, grip strength of each paw was analyzed using a wire, 3 mm in diameter, to determine grip strength scores ranging from 0 to 3 (0 normal grip strength, 1 mildly reduced grip strength, 2 moderately reduced grip strength, and 3 severely reduced grip strength). Assessments were performed in a blinded fashion. Animals were killed at week 10 after disease induction.

2.3. Evaluation of inflammation and local bone erosions by histologic examination

Mouse hind paws were fixed in formalin for 6 h, decalcified in 14% EDTA/ammonium hydroxide buffer until the bones were pliable. Serial paraffin sections (2 μm) were stained with hematoxylin and eosin (H&E) or stained for tartrate-resistant acid phosphatase (TRAP) activity. TRAP staining was performed using a leukocyte acid phosphatase staining kit (Sigma). For exact quantification of the areas of inflammation and erosions, H&E− and TRAP-stained sections were evaluated using an Axioskop 2 microscope (Carl Zeiss Micro- Imaging) and Osteomeasure Analysis System (OsteoMetrics), which allows absolute quantification of areas in histologic sections. The sum of the inflamed or eroded areas of inflammation for each single mouse was calculated by evaluating all tarsal joints. In addition, the number of osteoclasts was counted on TRAP-stained serial sections.

2.4. Measurement of serum anti-collagen type II antibody levels

On day 21 and day 60 after the first immunization, approximately 50 μl of blood of each animal was collected from the tail vein. Serum samples were prepared and anti-collagen type II (CII) antibody levels were determined by ELISA. Isolated sera were investigated for total *anti*-CII IgM and IgG, as well as for *anti*-CII IgG1 and IgG2c levels through quantitative ELISA as described previously [22]. Plates were coated with rat CII (10 μg/ml) in PBS overnight. After washing 3 times with PBS/Tween, the diluted serum samples were added and incubated for 2 h at room temperature or overnight at 4 °C. After washing plates 5 times, peroxidase-conjugated rat anti-mouse IgG or goat anti-mouse antibodies specific for IgM, IgG1 and IgG2c (Southern Biotech) were used as detecting antibodies. Plates were developed using ABTS (Roche Diagnostic Systems) as substrate, and the absorbance was then measured at 405 nm using a Synergy-2 reader (BioTek). Total *anti*-CII IgG levels were measured as μg/ml using purified polyclonal *anti*-CII IgG antibodies of a known concentration as a standard. For IgM and IgG-isotype levels, sera were pre-diluted 1:500 in duplicates and OD values were determined using pooled sera from naive and arthritic mice as negative and positive control, respectively.

2.5. TNP- KLH immunization

20 μg TNP- keyhole limpet hemocyanin (KLH) (Biosearch Technologies) was allowed to adsorb on 2 mg of aluminum hydroxide (Thermofisher) for 1 h at 4 °C. Non-adsorbed TNP-KLH was washed away with PBS, the TNP-KLH-aluminum hydroxide mixture was resuspended in 200 μl PBS and injected intraperitoneally. TNP-specific serum titers were determined 10 days later by ELISA as follows: briefly, 96-well flat-bottom Immulon plates were coated with 100 μg/ml of TNP-BSA (Biosearch Technologies) overnight at 4 °C, washed with PBS, and blocked with PBS/1% BSA for 2 h at room temperature (RT). Antibody-containing serum diluted between 1/100 to 1/1000 was added to each well. Plates were incubated for 2 h at RT. Wells were washed with PBS/0,5% Tween-20. Plates were further incubated with a 1/2000 dilution of alkaline phosphatase-conjugated goat anti-mouse IgM or IgG1 antibody (Southern Biotechnology). 6 mice were

immunized per genotype.

2.6. Purification of mouse CD4$^+$ T cells

Pooled cell suspensions of lymph nodes (LN) and spleens were incubated with biotinylated anti-mouse CD11b (clone M1/70, BioLegends), anti-mouse CD8α (53–6.7, BD Biosciences), anti-mouse CD11c (HL, BD Biosciences), anti-mouse B220 (RA3-6B2, BioLegends), anti-mouse Gr1 (Ly-6g, BioLegends), anti-mouse NK1.1 (PK136, BioLegends) and anti-mouse Ter-119 (Ter-119, BD Biosciences) in PBS/2%FBS. CD4$^+$ T cells were purified by negative depletion using streptavidin beads (BD Biosciences) according to the manufacturer's instructions. CD4$^+$ T cells were further sorted into naive CD4$^+$ T cells (CD25$^-$CD44^{low}CD62L$^+$) on a FACS Aria cytometer (BD Biosciences). The purity of the populations was routinely > 99%.

2.7. Culturing and analysis of mouse CD4$^+$ T cells

FACS-sorted naive CD4$^+$ T cells were stimulated (day 0) with plate-bound anti-CD3ε (1 μg/ml) and anti-CD28 (3 μg/ml) (both BD) on 48-well plates (0.3 × 10^6 cells/well) in 1 ml T cell medium (RPMI GlutaMAX-I, supplemented with 10% FCS, antibiotics, and 2-mercaptoethanol; all from Sigma Aldrich) in the presence of 1 ng/ml TGF-β and/or 20 ng/ml IL-6 (R&D Systems). When indicated MS-275 (Selleckchem) (2 or 4 μM final concentration) or DMSO only (as carrier control) was added 48 h later and cells were cultured for additional 24 h. Cells were harvested and analyzed on day 3 of culture and incubated with Fc-Block (1:250, BD Biosciences) followed by surface staining. Dead cells were excluded with Fixable Viability Dye eFluor® 506 (eBioscience) according to the manufacturer's protocol. Cells were measured with BD Fortessa or BD LSRII cytometers and analyzed using FlowJo software (BD). The following antibodies were used: CD4 (RM4-5), TCRβ (H57-597) (all from eBioscience) and CCR6 (140706) (BD Bioscience).

2.8. Purification, culturing and analysis of human CD4$^+$ T cells

PBMC were isolated from heparinized blood by layering over LSM 1077 Lymphocyte Separation Medium (Biocoll Separation Medium, Merck Millipore)with density gradient centrifugation at 400×*g*. Cells were extracellularly stained for CD3 (SK7,BD Pharmigen), CD4 (REA623), CD45RA (HI100) both from Miltenyi Biotec, CD25 (M-A251, BD Pharmigen) and CD127 (eBioRDR5,ebioscience); followed by FACS-sorting for naive (CD45RA$^+$CD127^{hi}CD25^{neg}) CD3$^+$CD4$^+$ T cells on a BD FACSAria Fusion (BD Biosciences) cell sorter. FACS-sorted naive CD4$^+$ T cells were stimulated with human T-activator CD3/CD28 Dynabeads (Gibco Thermo Scientific) at a 1:1 ratio on 96-well plates (75000 cells/well) in 200 μL AIM V medium/well (Gibco) supplemented with 5 ng/ml TGF-β and/or 25 ng/ml IL-6 for 7 days, in the last 48 h in the presence of DMSO and 2 μM MS-275. Approximately, 0.5 × 10^6 cells were used for surface staining, dead cells were excluded using Fixable Viability Dye eFluor® 506 (Thermo Scientific) according to the manufacturer's protocol. The following antibodies were used: CD4 (RPA-T4), CD45RO (UCHL1) and CCR6 (REA190, Miltenyi Biotec).

2.9. Measurement of serum cytokines

Serum samples were collected before immunization (day −7), as well as 10 days and 55 days after immunization. IFN-γ, IL-10, IL-22, TNF-α, IL-6 and IL-17 were analyzed by LEGENDPlex (Biolegend) according to the manufacturer's instructions.

2.10. Statistical analysis

Statistical analyses were performed using Prism Software (GraphPad Inc) and R [23]. P-values were calculated with an unpaired two-tailed Student's t-test for normal distributed data with equal variances, Welch's *t*-test for normal distributed data with unequal variances, Wilcoxon test for non-normal distributed data and with Pearson's product moment correlation coefficient for correlations (the latter as implemented in 'cor.test' in R). No data were excluded. For CIA scoring, blinding of investigators was applied.

2.11. RNA-sequencing - data processing

RNA-seq from previously published data were analyzed as follows: reads were mapped either onto the mouse reference genome release mm10 (GRCm38) or onto the human reference genome release GRCh38 [24] with Ensembl transcript annotation version 89 [25] using Tophat version 2.1.1 [26] with Bowtie version 2.2.9 [27]. Reads were counted with featureCounts [28]. Gene expression values (fragments per kilobase exon per million mapped reads (FPKM)) were calculated with Cufflinks version 2.2 [29]. The differential expression between two paired sample groups was calculated with edgeR [30]. The filtering for differentially expressed genes is for p-value of 0.05 (FDR corrected) and minimal fold-change of 2. RNA-seq data of *WT* and Stat3$^{-/-}$ CD4$^+$ T cells are available on the GEO repository under the accession number GSE65621 [31].

2.12. Immunofluorescence staining of human RA synovial tissue samples

RA synovial tissues were obtained as discarded specimens following synovectomy or joint replacement with approval of the local ethics committee. Synovial tissues were frozen in TissueTEK compound (Sakura) and cryosections were made in 3 μm thickness. Sections were fixed with phosphate buffered formaldehyde, blocked with fetal calf serum and then incubated with the following antibodies: mouse anti-human-HDAC1 (10E2) (Cell Signaling Technology), rabbit anti-human-CCR6 (Lifespan Bioscience), Alexa Fluor 488 anti-human CD4 (Biolegend), Alexa Fluor 555 goat anti-mouse (Invitrogen) and Alexa Fluor 647 goat anti-rabbit (Invitrogen). Nuclei were counterstained with DAPI (Molecular Probes). Slides were mounted using ProLong Gold antifade reagent (Molecular Probes). Images were acquired using an Olympus IX83 microscope and analyzed with Cell Profiler Version 3.1.5..

3. Results

3.1. HDAC1-cKO mice are resistant to CIA

To test the importance of HDAC1 in CD4$^+$ T cells for the development of CIA, we immunized *Hdac1$^{flox/flox}$xCd4^{Cre}* (*HDAC1-cKO*) and Hdac1$^{flox/flox}$ mice (*WT)* control mice with chicken collagen type II,in complete Freund's adjuvant (CFA) as described previously [2,19]. Mice were evaluated twice a week for the development of arthritis by a semi-quantitative score, that includes paw swelling and grip strength. *WT* mice developed clear clinical signs of arthritis, such as paw swelling and reduced grip strength. Surprisingly, *HDAC1-cKO* mice were completely protected from CIA (Fig. 1a and Supplementary Fig. 1)). Detailed histological analysis of the paws of *WT* mice showed severe signs of arthritis including inflammation, erosion and infiltration of osteoclasts, while *HDAC1-cKO* mice did not show any histological signs of inflammation (Fig. 1b and c). Thus, deletion of HDAC1 in T cells inhibits the development of arthritis.

3.2. HDAC1-cKO mice show an unaltered antibody response

Since CIA is characterized by increased production of pathogenic autoantibodies, we measured anti-collagen II (*anti*-CII) antibody levels in the sera of immunized *HDAC1-cKO* and *WT* mice. In line with the clinical data, *WT* mice developed *anti*-CII antibody at day 21 after immunization. Unexpectedly, although *HDAC1-cKO* mice did not develop

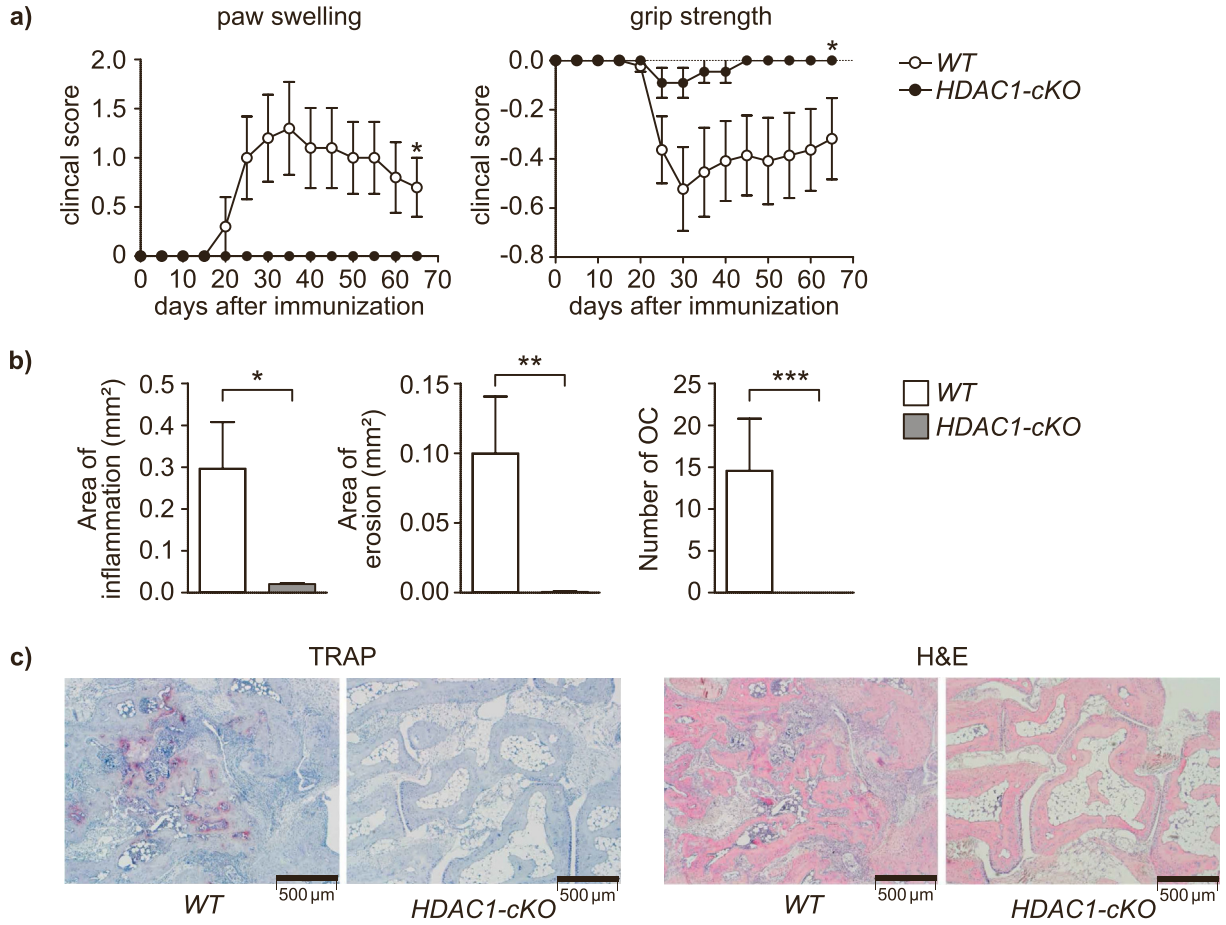

Fig. 1. Loss of HDAC1 protects from the development of CIA. CIA was induced in *WT* and *HDAC1-cKO* mice **a)** Clinical quantification of paw swelling and grip strength in *WT* (n = 11) and *HDAC1-cKO* mice (n = 12) after induction of CIA. Data are expressed as Mean values ± Standard Error of the Mean. Data show one representative out of two independent experiments. Significant differences could be detected for paw swelling and grip strength using a two-way anova *p ≤ 0.05 **b)** At week 10 mice were sacrificed and analyzed for histological signs of inflammation. Plots show quantitative histomorphometric analysis of hind paws of *WT* and *HDAC1-cKO* mice after CIA induction. Data are expressed as Mean values ± Standard Error of the Mean. Statistical significance is shown as asterisks *p ≤ 0.05, **p ≤ 0.01, ***p ≤ 0.001. **c)** Representative TRAP and H&E stainings from histological sections are shown from *WT* and *HDAC1-cKO* mice.

arthritis, similar amounts of total *anti*-CII IgG and *anti*-CII IgM were detected (Fig. 2a) as compared to *WT* mice. In particular, no difference could be detected for the levels of the *anti*-CII IgG subclasses IgG1 and IgG2c, which are known to be pathogenic isotypes in the CIA model (Fig. 2a). These data suggest an unaltered inflammatory cascade in response to immunization with chicken collagen type II and CFA.

To further investigate the T cell-dependent antibody response, we immunized *WT* and *HDAC1-cKO* mice with the thymus-dependent antigen TNP-KLH. In line with the data obtained in the CIA model, no differences in the titers of IgM and IgG1 antibodies specific to TNP after immunization with a TNP-KLH-aluminum hydroxide mixture were observed in *HDAC1-cKO* compared to *WT* mice measured ten days after intraperitoneal immunization (Fig. 2b).

This suggests an undisturbed T cell/B cell interaction in the absence of HDAC1 and an unimpaired antibody switch to IgG1 in *HDAC1-cKO* mice. Collectively, these data implicate an undisturbed T cell-mediated B cell response in *HDAC1-cKO* mice.

3.3. Diminished Th17 cytokines in HDAC1-cKO mice

Various cytokines have been described to play a crucial role for the development of CIA and display potent therapeutic targets [32]. To analyze potential alterations in the cytokine milieu in the absence of HDAC1, we measured serum cytokines in chicken CII/CFA-immunized *WT* and *HDAC1-cKO* mice. On day 10 after immunization we observed a strong upregulation of inflammatory cytokine production (TNF-α, IFN-γ, IL-6 and IL-17) in *WT* as well as *HDAC1-cKO* mice when compared to pre-immunized *WT* and *HDAC1-cKO* mice, respectively. No difference was detected for the Th1-associated cytokines IFN-γ and TNF-α or other cytokines such as IL-10 and IL-22 (Fig. 3). Interestingly, IL-6 and IL-17 were significantly reduced in *HDAC1-cKO* mice as compared to *WT* mice (Fig. 3), suggesting a role of HDAC1 in the regulation of Th17-associated pathways under inflammatory conditions.

3.4. Disturbed regulation of CCR6 in HDAC1-cKO mice

To define the Th17-associated signature we compared the transcriptome of ex vivo isolated naive $CD4^+$ T cells and IL-17 GFP^+ Th17 cells, isolated from lamina propria cells, from previously published datasets [33]. As depicted in Fig. 4a we observed a high number of differentially regulated genes in ex vivo isolated Th17 cells as compared to naive $CD4^+$ T cells. Among them, Ccr6 was highly upregulated in differentiated Th17 cells (Fig. 4b). Since IL-6 is a major driver of Th17 cells and is diminished in the serum of *HDAC1-cKO* mice (Fig. 3) we addressed the effects of IL-6 on $CD4^+$ T cells. Naive $CD4^+$ T cells ($CD44^{lo}CD62L^+CD25^-$) from *WT* and *HDAC1-cKO* mice were activated via anti-CD3 and anti-CD28 and cultured in the presence of IL-6 for 3 days. Surprisingly, IL-6 stimulated $CD4^+$ T cells from *WT* mice revealed a strong expression of CCR6, which is a crucial chemokine receptor for the development of CIA [3,19]. In contrast, HDAC1-deficient $CD4^+$ T

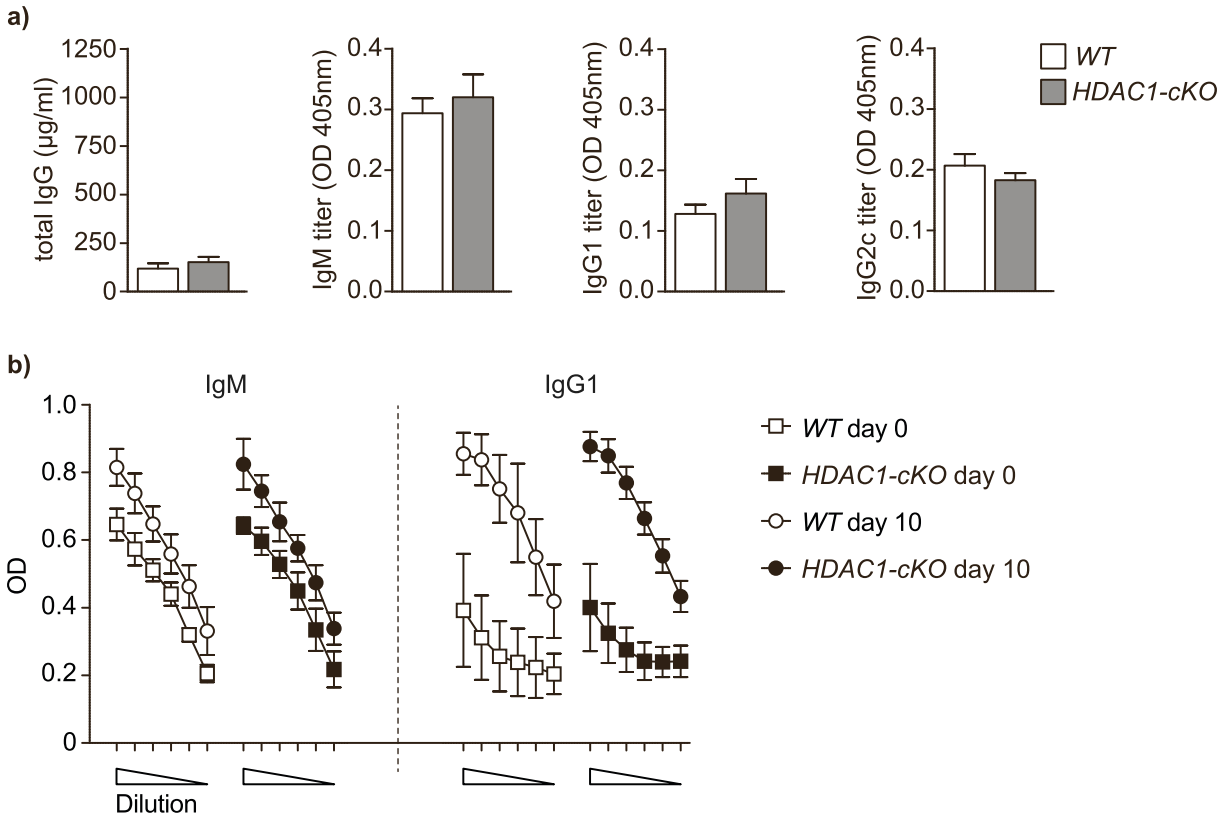

Fig. 2. Regular antibody production in *HDAC1-cKO* mice a) *Anti*-CII antibodies from the serum of *WT* and *HDAC1-cKO* mice were measured by ELISA at day 21 after induction of CIA. Total *anti*-CII IgG antibody concentration is shown in µg/ml. IgM and IgG isotype levels are presented in levels of OD 405 signal. Data are expressed as Mean values ± Standard Error of the Mean. **b)** Mice were immunized with TNP-KLH in aluminum hydroxide mixed with PBS on day 0 (n = 6 per group). At day 10, IgM and IgG1 isotype levels were evaluated by antigen-specific ELISA. Mean values ± Standard Deviation Data show the summary **(a)** of 11 WT and 11 *HDAC1-cKO* mice that were analyzed in one experiment or show one representative of two independent experiments of 6 WT and 6 *HDAC1-cKO* mice **(b)**.

cells failed to express CCR6 under this condition (Fig. 4c), similar to observations previously made in anti-CD3/anti-CD28 (Th0) activated HDAC1-cKO CD4$^+$ T cells [34]. IL-6 exerts its effect mainly through signal transducer and activator of transcription 3 (STAT) 3 and STAT1 [4,31]. Analysis of previously published STAT3 ChIP-Seq datasets [4,31] revealed multiple binding peaks in the *Ccr6* gene locus in naive CD4$^+$ T cells in the presence of IL-6 (Fig. 4d), strongly suggesting that STAT3 is part of the transcriptional network regulating of *Ccr6* expression. In line with this, *Ccr6* mRNA levels were significantly diminished in *Stat3*$^{-/-}$ mice (Fig. 4e). To further investigate the effects of selective HDACi on the *in vitro* differentiation of Th17 cells we isolated naive *WT* CD4$^+$ T cells and stimulated them with IL-6 and TGF- β

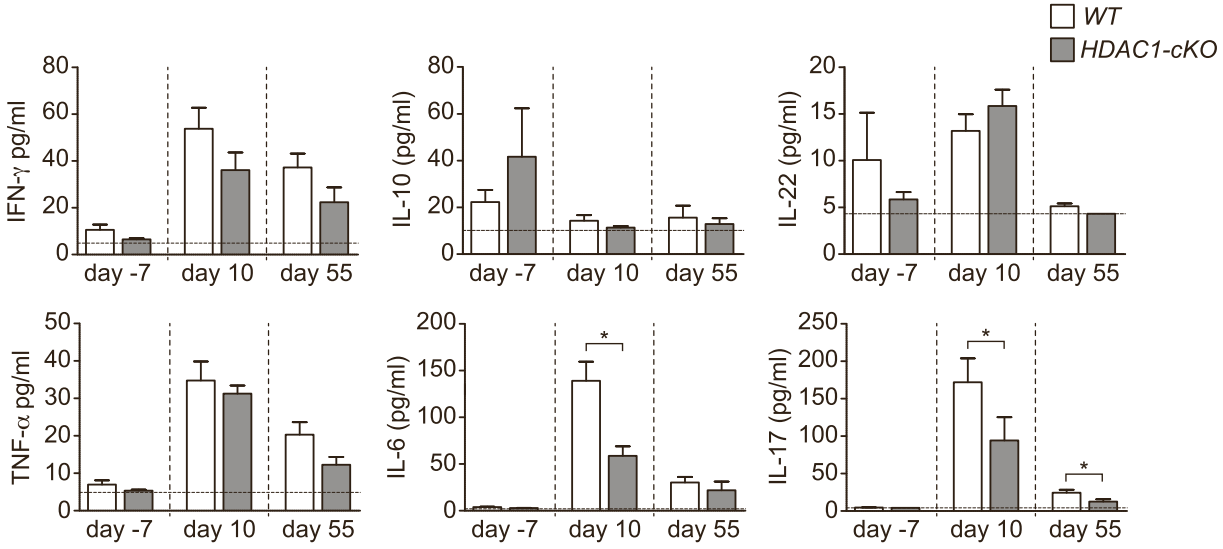

Fig. 3. Diminished production of pro-inflammatory cytokines in *HDAC1-cKO* mice. Serum cytokines were measured before (day −7) and after induction of CIA (day 10 and day 55) by flow cytometry. Statistical significance is shown as asterisks *p ≤ 0.05. Data are expressed as Mean values ± Standard Error of the Mean. Data show the summary of 12 WT mice and 12 *HDAC1-cKO* mice analyzed in one experiment.

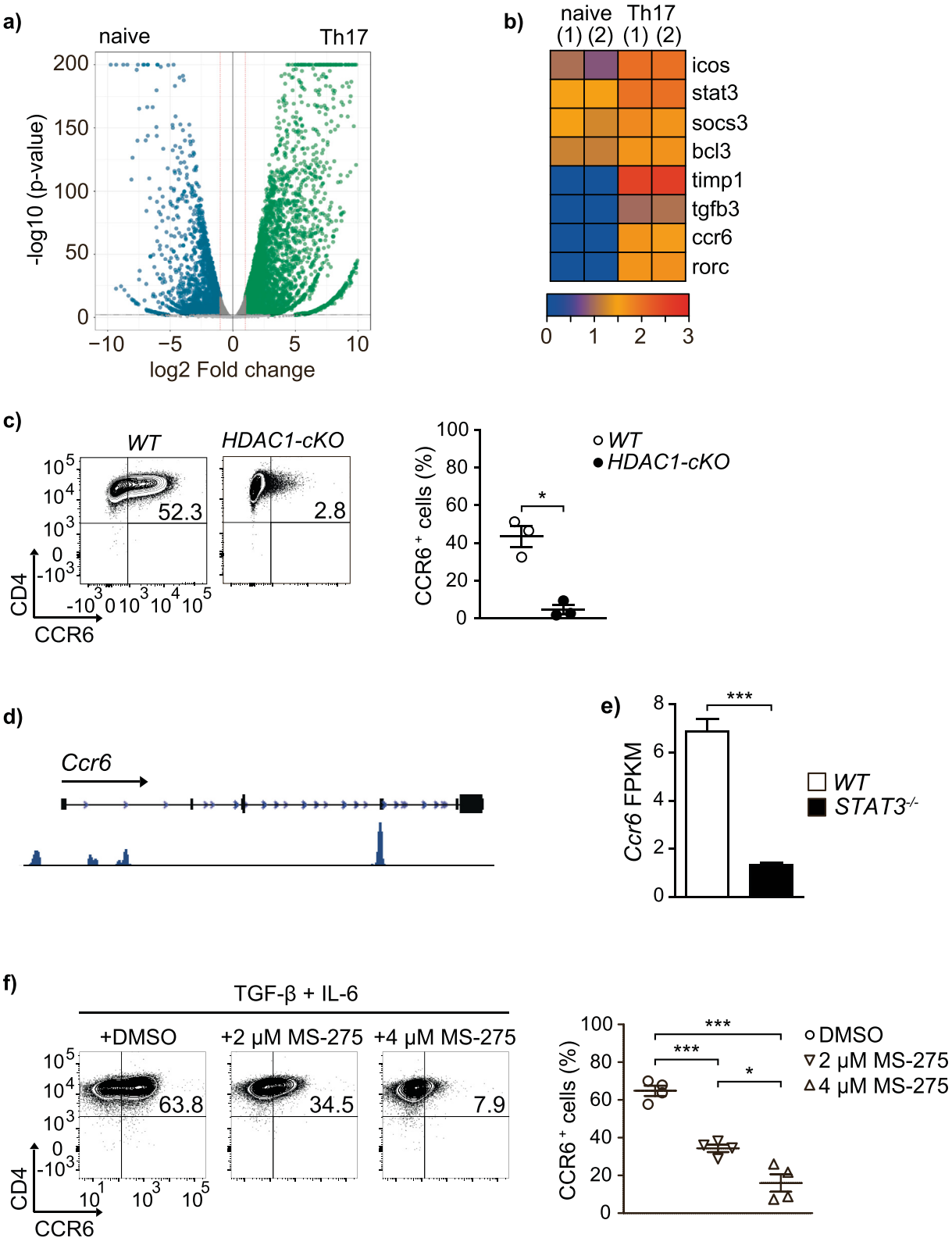

(caption on next page)

in the presence or absence of the class I HDAC inhibitor MS-275 [35]. We observed a dose-dependent reduction of CCR6 expression under Th17 skewing conditions (Fig. 4f). These data support a key role of CCR6 as a target of selective HDACi in CD4$^+$ T cells.

3.5. Disturbed regulation of CCR6 in CD4$^+$ T cells from RA patients

To further investigate a potential link between RA and class I HDACs, we determined the expression levels of HDAC1 in samples from human RA patients. We combined a collection of RNA-seq datasets of synovial biopsies from healthy individuals and untreated newly

Fig. 4. HDAC1 affects CCR6 expression. Previously published RNA-seq datasets from naïve T cells, isolated from the spleen and IL-17 GFP$^+$ Th17 cells, isolated from lamina propria cells, were re-analyzed [33]. **a)** Differentially regulated genes are shown as volcano plot. The thresholds for (significantly) different expression are a maximal FDR of 0.05 and a minimal fold-change of 2 in either direction with 5579 up-regulated and 4361 down-regulated genes. **b)** log10 FPKM expression values of Th17 signature genes are compared in naive and Th17 cells, shown as a heat map. The range for log10 FPKMs is set from 0 to 3, values outside this range are set to the limits. **c)** Naive CD4$^+$ T cells from *WT* and *HDAC1-cKO* mice were activated with anti-CD3/anti-CD28 for 3 days in the presence of IL-6 (20 ng/ml). Expression of CCR6 was measured by flow cytometry. The summary is showing the percentage of CCR6$^+$ cells. Each plot represents one mouse analyzed in 3 independent experiments. **d)** STAT3 ChIP-Seq as well as RNA-seq was performed on IL-6 treated naive CD4$^+$ T cells as described by Hirahara et al. [31]. One representative screen shot of the *Ccr6* gene locus is shown. **e)** RNA-seq was performed in activated *WT* and *STAT3*$^{-/-}$ CD4$^+$ T cells when cultured in the presence of IL-6 for 3 days. (as described by Hirahara et al. [31]. RNA-seq FPKM values of Ccr6 expression are shown (n = 3). Mean values ± Standard Error of the mean are shown. **f)** Naive CD4$^+$ T cells from WT mice were stimulated with anti-CD3/anti-CD28 under Th17-polarizing conditions (IL-6 + TGF-β) in the presence of MS-275 or DMSO control. Expression of CCR6 was analyzed on day 3 by flow cytometry. When indicated, statistical significance was shown as asterisks; *p ≤ 0.05, **p ≤ 0.01, ***p ≤ 0.001.

diagnosed RA patients from previously published datasets [36]. Indeed, we observed increased levels of HDAC1 in RA patients as compared to HC consistent with elevated levels of CD4$^+$ T cells, which positively correlated to HDAC1 expression levels (Fig. 5a and b). In addition, HDAC1 expression levels also correlated with CCR6 expression levels (Supplementary Fig. 2a). We further stained synovial tissue samples from RA patients for CD4, CCR6 and HDAC1 and revealed a co-localization of CCR6, HDAC1 and CD4 (Fig. 5c), indicating the presence of a CD4$^+$CCR6$^+$HDAC1$^+$ T cell population in the synovial tissue of RA patients.

To test the impact of HDAC inhibitors on the expression of CCR6, we isolated human CD4$^+$ T cells from healthy controls (HC) and cultured them in the presence of TGF- β and IL-6 and MS-275 (or DMSO as carrier control). In line with the murine data (Fig. 4f) we observed a decrease of CCR6 expression upon MS-275 treatment. To further underline the relevance of selective HDAC inhibition on CCR6 levels, we analyzed published RNA-seq data [37] of CD4$^+$ T cells isolated from patients with cutaneous T cell lymphoma under treatment with the HDACi vorinostat or romidepsin. As shown in Supplementary Fig. 2b, CD4$^+$ T cells display reduced CCR6 expression over the time of treatment. These data are in agreement with our *in vitro* data and highlight the potential of selective HDACi for patients with Th17-driven autoimmune diseases.

4. Discussion

Herein we addressed the role of HDAC1 in T cells for the development of arthritis in the CIA model, which is still one of the most widely used experimental models of RA. The anti-inflammatory effects of various non-selective HDACi have been described in additional murine arthritis models, which suggests a potential use for treatment of inflammatory and autoimmune diseases [6–17,38,39]. To focus on the selective role of HDACs, *Hdac1*$^{flox/flox}$ mice were crossed to *Cd4*^{Cre} mice, which allowed us to investigate the effects of HDAC1 in CD4$^+$ T cells under inflammatory conditions. Remarkably, *HDAC1-cKO* mice were completely protected from the development of arthritis and did not show any clinical or histological signs of disease.

Measurement of *anti*-CII antibody serum levels revealed no difference between *WT* and *HDAC-1cKO* mice. In line with the unimpaired production of *anti*-CII antibodies, we detected no differences in TNP-specific antibody subclasses between *HDAC1-cKO* and *WT* mice. This strongly suggests an intact T cell-mediated B cell response, which is indispensable for the development of CIA [40]. Since the induction of CIA is dependent on effector CD4$^+$ T cells, we measured Th1, Th2 and Th17-dependent cytokines in the serum. A strong upregulation of pro-inflammatory cytokines after immunization was found in both *WT* and *HDAC1-cKO* mice, which reflects the undisturbed first wave of the immune response. Interestingly, Th17 signature cytokines, such as IL-6 and IL-17, were significantly decreased in *HDAC1-cKO* mice. IL-17A is secreted by Th17 cells which express the transcription factor RAR-related orphan receptor-C (RORC) and the chemokine receptor CCR6 [41,42]. Since the discovery of Th17 cells, an overwhelming number of studies have been published, which highlights the potential role of this subset for the pathogenesis of RA [43]. In RA patients increased numbers of CD4$^+$ T cells expressing CCR6 were found among PBMCs as well as in the inflamed synovium. In addition, our group could recently demonstrate that *Ccr6*$^{-/-}$ mice develop a less severe arthritis in the CIA model [19]. Our data show a severe dysregulation of CCR6 expression in IL-6 stimulated HDAC1 deficient CD4$^+$ T cells in a STAT3 dependent manner. These data are in line with our previously published data which show that CCR6 expression in anti-CD3/anti-CD28 activated CD4$^+$ T cells is diminished in the absence of HDAC1 [34]. Accordingly, selective inhibition of class I HDACs leads to a dose-dependent inhibition of CCR6 expression under Th17 polarizing conditions in mouse and human CD4$^+$ T cells. Of note, *HDAC1-cKO* CD4$^+$ T cells cultured in the presence of TGF-β and IL-6 did not display a reduced expression of CCR6 [34], suggesting that other HDACs might compensate for loss of HDAC1. We conclude that disturbed CCR6 regulation in *HDAC1-cKO* mice might impair the migration of CD4$^+$ T cells, which affects severity of arthritis in *HDAC1-cKO* mice. This assumption is strongly supported by our previous analysis of CIA in *Ccr6*$^{-/-}$ mice, which also show reduced levels of arthritis. Since the reduction of arthritis is even more pronounced in mice with a germline deletion of *Ccr6*, additional cell subsets other then CD4$^+$ T cells, which also express CCR6, most likely contribute to the development of CIA. To provide a further rationale for the role of HDACs in the pathogenesis of RA we analyzed expression levels of HDAC1 in CD4$^+$CCR6$^+$ T cells from existing RNA-seq data and performed histological analysis of human synovial tissue samples. HDAC1 levels were elevated in RA patients as compared to HC and correlated with the number of CD4$^+$ T cells. Accordingly, we observed CD4$^+$CCR6$^+$HDAC1$^+$ T cells in synovial tissue samples, which suggests a role of HDAC1 also in the pathogenesis of RA. Th17 polarization of murine and human T cells in the presence of a selective HDAC inhibitor also decreased CCR6 expression. These data are in line with the existing literature which shows that HDACi have effects on various cell types from RA patients, including peripheral blood mononuclear PBMCs, macrophages and FLS [6–8,11–17,44]. To confirm CCR6 as a treatment target for HDACi, we reanalyzed RNA-seq data from CD4$^+$ T cells from patients suffering from cutaneous T cell lymphoma under treatment with vorinostat and romidepsin [37]. Indeed, also in ex vivo isolated human samples inhibition of HDACs had a direct effect on the expression of CCR6 in CD4$^+$ T cells. These data highlight the role of CD4$^+$ cells and elucidate the importance of HDAC1 for the development of arthritis. Furthermore, we could identify CCR6 as a treatment target of HDACi. Selective inhibition of class I HDACs might therefore be a promising new treatment option for Th17-mediated autoimmune diseases.

CRediT authorship contribution statement

Lisa Göschl: Conceptualization, Data curation, Formal analysis, Investigation, Methodology, Software, Visualization, Writing - original draft. **Teresa Preglej:** Methodology. **Nicole Boucheron:** Funding acquisition, Methodology. **Victoria Saferding:** Methodology. **Lena Müller:** Methodology. **Alexander Platzer:** Formal analysis, Software, Visualization. **Kiyoshi Hirahara:** Formal analysis, Visualization. **Han-Yu Shih:** Formal analysis, Visualization. **Johan Backlund:** Methodology. **Patrick Matthias:** Resources. **Birgit Niederreiter:**

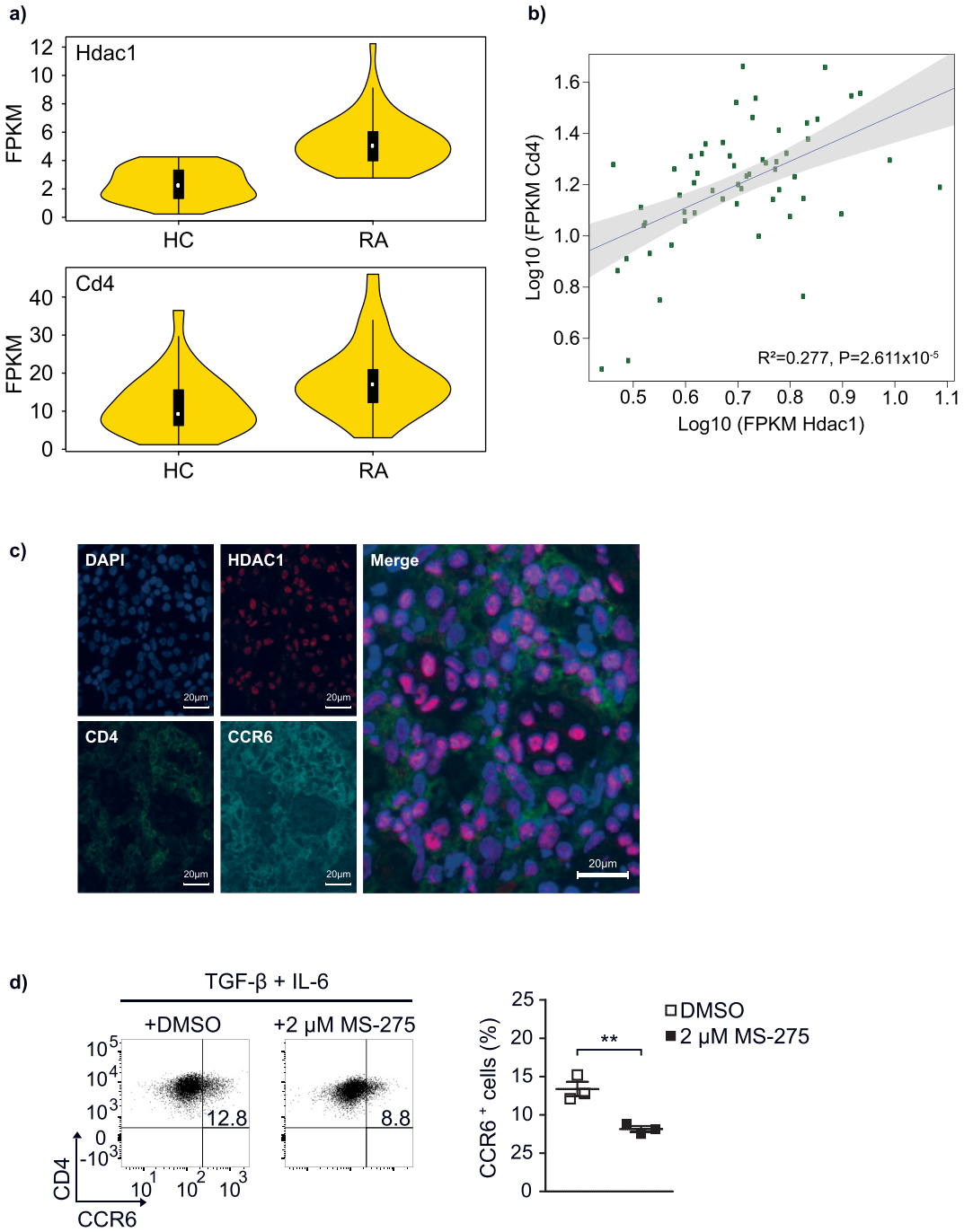

Fig. 5. HDAC1 expression in T cells from RA patients. Gene expression of Cd4 and Hdac1 of previously published and analyzed RNA-seq data from synovial biopsies [36,45] was compared between healthy subjects and patients with early RA. **a)** CD4 (p-value = 0.000985) and HDAC1 (p-value = $1.575 * 10^{-10}$) were significantly elevated in early diagnosed untreated RA patients as compared to HC. **b)** CD4 expression is significantly correlated to HDAC1 expression ($R^2 = 0.277$, p-value = 2.611*^10^{-5}). **c)** Synovial tissue samples from RA patients were stained for the expression of CD4, CCR6 and HDAC1. Nuclei were stained for DAPI. One representative example out of 6 is shown. **d)** Naive $CD3^+CD4^+$ $CD45RA^+CD127^{hi}CD25^{neg}$ T cells from HC were activated in the presence of TGF-β and MS-275 or DMSO control. After 7 days CCR6 expression was analyzed by flow cytometry. When indicated, statistical significance was shown as asterisks; *p ≤ 0.05, **p ≤ 0.01, ***p ≤ 0.001.

Methodology. **Anastasiya Hladik:** Methodology. **Maximilian Kugler:** Software. **Guido A. Gualdoni:** Resources. **Clemens Scheinecker:** Resources, Writing - review & editing. **Sylvia Knapp:** Resources. **Christian Seiser:** Resources. **Rikard Holmdahl:** Writing - review & editing. **Katharina Tillmann:** Resources. **Roberto Plasenzotti:** Resources. **Bruno Podesser:** Resources. **Daniel Aletaha:** Writing - review & editing. **Josef S. Smolen:** Writing - review & editing. **Thomas Karonitsch:** Formal analysis. **Günter Steiner:** Funding acquisition, Resources, Writing - review & editing. **Wilfried Ellmeier:** Funding acquisition, Resources, Writing - review & editing. **Michael Bonelli:** Conceptualization, Data curation, Funding acquisition, Project administration, Supervision, Validation, Writing - original draft.

Declaration of competing interest

None.

This research has received support from the Innovative Medicines Initiative (IMI) Joint Undertaking under grant *agreement* n°115142 (BTCure), and grant agreement n° 777357 (RTCure) resources of which are composed of financial contribution from the European Union's Framework Programmes and EFPIA companies' in kind contribution. The work has been supported by the Austrian Science Fund (FWF) project F26193 (to WE) and the FWF special research program SFB F70 (subproject F7003 to MB, F7004 to NB and F7005 to WE).

Acknowledgement

We thank Brigitte Meyer, Carl-Walter Steiner and Tetyana Shvets for expert technical assistance.

Appendix A. Supplementary data

Supplementary data to this article can be found online at https://doi.org/10.1016/j.jaut.2019.102379.

References

[1] J.S. Smolen, D. Aletaha, I.B. McInnes, Rheumatoid arthritis, Lancet 388 (2016) 2023–2038, https://doi.org/10.1016/S0140-6736(16)30173-8.
[2] W. de Jager, E.P.A.H. Hoppenreijs, N.M. Wulffraat, L.R. Wedderburn, W. Kuis, B.J. Prakken, Blood and synovial fluid cytokine signatures in patients with juvenile idiopathic arthritis: a cross-sectional study, Ann. Rheum. Dis. 66 (2007) 589–598, https://doi.org/10.1136/ard.2006.061853.
[3] Y. Kanno, G. Vahedi, K. Hirahara, K. Singleton, J.J. O'Shea, Transcriptional and epigenetic control of T helper cell specification: molecular mechanisms underlying commitment and plasticity *, Annu. Rev. Immunol. 30 (2012) 707–731, https://doi.org/10.1146/annurev-immunol-020711-075058.
[4] M. Haberland, R.L. Montgomery, E.N. Olson, The many roles of histone deacetylases in development and physiology: implications for disease and therapy, Nat. Rev. Genet. 10 (2009) 32–42, https://doi.org/10.1038/nrg2485.
[5] W. Ellmeier, C. Seiser, Histone deacetylase function in CD4, Nat. Rev. Immunol. (2018) 1–18, https://doi.org/10.1038/s41577-018-0037-z.
[6] A.M. Grabiec, S. Krausz, W. de Jager, T. Burakowski, D. Groot, M.E. Sanders, et al., Histone deacetylase inhibitors suppress inflammatory activation of rheumatoid arthritis patient synovial macrophages and tissue, J. Immunol. 184 (2010) 2718–2728, https://doi.org/10.4049/jimmunol.0901467.
[7] A.M. Grabiec, O. Korchynskyi, P.P. Tak, K.A. Reedquist, Histone deacetylase inhibitors suppress rheumatoid arthritis fibroblast-like synoviocyte and macrophage IL-6 production by accelerating mRNA decay, Ann. Rheum. Dis. 71 (2012) 424–431, https://doi.org/10.1136/ard.2011.154211.
[8] J. Gillespie, S. Savic, C. Wong, A. Hempshall, M. Inman, P. Emery, et al., Histone deacetylases are dysregulated in rheumatoid arthritis and a novel histone deacetylase 3-selective inhibitor reduces interleukin-6 production by peripheral blood mononuclear cells from rheumatoid arthritis patients, Arthritis Rheum. 64 (2012) 418–422, https://doi.org/10.1002/art.33382.
[9] T. Kawabata, K. Nishida, K. Takasugi, H. Ogawa, K. Sada, Y. Kadota, et al., Increased activity and expression of histone deacetylase 1 in relation to tumor necrosis factor-alpha in synovial tissue of rheumatoid arthritis, Arthritis Res. Ther. 12 (2010) R133, https://doi.org/10.1186/ar3071.
[10] C. Angiolilli, A.M. Grabiec, B.S. Ferguson, C. Ospelt, B. Malvar Fernandez, I.E. van Es, et al., Inflammatory cytokines epigenetically regulate rheumatoid arthritis fibroblast-like synoviocyte activation by suppressing HDAC5 expression, Ann. Rheum. Dis. 75 (2016) 430–438, https://doi.org/10.1136/annrheumdis-2014-205635.
[11] B.R. Oh, D.-H. Suh, D. Bae, N. Ha, Y. Il Choi, H.J. Yoo, et al., Therapeutic Effect of a Novel Histonedeacetylase 6 Inhibitor, CKD-L, on Collagen-Induced Arthritis in Vivo and regulatoryT Cells in Rheumatoid Arthritis in Vitro, (2017), pp. 1–16, https://doi.org/10.1186/s13075-017-1357-2.
[12] S. Hawtree, M. Muthana, J.M. Wilkinson, M. Akil, A.G. Wilson, Histone deacetylase 1 regulates tissue destruction in rheumatoid arthritis, Hum. Mol. Genet. 24 (2015) 5367–5377, https://doi.org/10.1093/hmg/ddv258.
[13] M.D. Cantley, D.P. Fairlie, P.M. Bartold, V. Marino, P.K. Gupta, D.R. Haynes, Inhibiting histone deacetylase 1 suppresses both inflammation and bone loss in arthritis, Rheumatology 54 (2015) 1713–1723, https://doi.org/10.1093/rheumatology/kev022.
[14] L. Joosten, F. Leoni, Mol. Med. 17 (2011) 1, https://doi.org/10.2119/molmed.2011.00058.
[15] S.J. Saouaf, B. Li, G. Zhang, Y. Shen, N. Furuuchi, W.W. Hancock, et al., Deacetylase inhibition increases regulatory T cell function and decreases incidence and severity of collagen-induced arthritis, Exp. Mol. Pathol. 87 (2009) 99–104, https://doi.org/10.1016/j.yexmp.2009.06.003.
[16] Y. Nasu, K. Nishida, S. Miyazawa, T. Komiyama, Y. Kadota, N. Abe, et al., Trichostatin A, a histone deacetylase inhibitor, suppresses synovial inflammation and subsequent cartilage destruction in a collagen antibody-induced arthritis mouse model, Osteoarthr. Cartil. 16 (2008) 723–732, https://doi.org/10.1016/j.joca.2007.10.014.
[17] H.-S. Lin, C.-Y. Hu, H.-Y. Chan, Y.-Y. Liew, H.-P. Huang, L. Lepescheux, et al., Anti-rheumatic activities of histone deacetylase (HDAC) inhibitors in vivoin collagen-induced arthritis in rodents, Br. J. Pharmacol. 150 (2007) 862–872, https://doi.org/10.1136/ard.61.suppl_2.ii67.
[18] L. Goschl, T. Preglej, P. Hamminger, M. Bonelli, L. Andersen, N. Boucheron, et al., J. Autoimmun. 86 (2018) 51–61, https://doi.org/10.1016/j.jaut.2017.09.008.
[19] M. Bonelli, A. Puchner, L. Goschl, S. Hayer, B. Niederreiter, G. Steiner, et al., CCR6 controls autoimmune but not innate immunity-driven experimental arthritis, J. Cell Mol. Med. 22 (2018) 5278–5285, https://doi.org/10.1186/s13075-015-0800-5.
[20] R. Grausenburger, I. Bilic, N. Boucheron, G. Zupkovitz, L. El-Housseiny, R. Tschismarov, et al., Conditional deletion of histone deacetylase 1 in T cells leads to enhanced airway inflammation and increased Th2 cytokine production, J. Immunol. 185 (2010) 3489–3497, https://doi.org/10.4049/jimmunol.0903610.
[21] J. Backlund, C. Li, E. Jansson, S. Carlsen, P. Merky, K.S. Nandakumar, et al., C57BL/6 mice need MHC class II Aq to develop collagen-induced arthritis dependent on autoreactive T cells, Ann. Rheum. Dis. 72 (2013) 1225–1232, https://doi.org/10.1136/annrheumdis-2012-202055.
[22] R. Holmdahl, L. Klareskog, M. Andersson, C. Hansen, High antibody response to autologous type II collagen is restricted to H-2q, Immunogenetics 24 (1986) 84–89.
[23] K.N. Kirby, D. Gerlanc, BootES: an R package for bootstrap confidence intervals on effect sizes, Behav. Res. Methods 45 (2013) 905–927, https://doi.org/10.3758/s13428-013-0330-5.
[24] M.L. Speir, A.S. Zweig, K.R. Rosenbloom, B.J. Raney, B. Paten, P. Nejad, et al., The UCSC Genome Browser database: 2016 update, Nucleic Acids Res. 44 (2016) D717–D725, https://doi.org/10.1093/nar/gkv1275.
[25] D.R. Zerbino, P. Achuthan, W. Akanni, M.R. Amode, D. Barrell, J. Bhai, et al., Ensembl 2018, Nucleic Acids Res. 46 (2018) D754–D761, https://doi.org/10.1093/nar/gkx1098.
[26] C. Trapnell, L. Pachter, S.L. Salzberg, TopHat: discovering splice junctions with RNA-Seq, Bioinformatics 25 (2009) 1105–1111, https://doi.org/10.1093/bioinformatics/btp120.
[27] B. Langmead, S.L. Salzberg, Fast gapped-read alignment with Bowtie 2, Nat. Methods 9 (2012) 357–359, https://doi.org/10.1038/nmeth.1923.
[28] Y. Liao, G.K. Smyth, W. Shi, featureCounts: an efficient general purpose program for assigning sequence reads to genomic features, Bioinformatics 30 (2014) 923–930, https://doi.org/10.1093/bioinformatics/btt656.
[29] C. Trapnell, B.A. Williams, G. Pertea, A. Mortazavi, G. Kwan, M.J. van Baren, et al., Transcript assembly and quantification by RNA-Seq reveals unannotated transcripts and isoform switching during cell differentiation, Nat. Biotechnol. 28 (2010) 511–515, https://doi.org/10.1038/nbt.1621.
[30] M.D. Robinson, D.J. McCarthy, G.K. Smyth, edgeR: a Bioconductor package for differential expression analysis of digital gene expression data, Bioinformatics 26 (2010) 139–140, https://doi.org/10.1093/bioinformatics/btp616.
[31] K. Hirahara, A. Onodera, A.V. Villarino, M. Bonelli, G. Sciumè, A. Laurence, et al., Asymmetric action of STAT transcription factors drives transcriptional outputs and cytokine specificity, Immunity 42 (2015) 877–889, https://doi.org/10.1016/j.immuni.2015.04.014.
[32] I.B. McInnes, C.D. Buckley, J.D. Isaacs, Cytokines in rheumatoid arthritis - shaping the immunological landscape, Nat. Rev. Rheumatol. 12 (2016) 63–68, https://doi.org/10.1038/nrrheum.2015.171.
[33] H.-Y. Shih, G. Sciumè, Y. Mikami, L. Guo, H.-W. Sun, S.R. Brooks, et al., Developmental acquisition of regulomes underlies innate lymphoid cell functionality, Cell 165 (2016) 1120–1133, https://doi.org/10.1016/j.cell.2016.04.029.
[34] L. Goschl, T. Preglej, P. Hamminger, M. Bonelli, L. Andersen, N. Boucheron, et al., J. Autoimmun. 86 (2018) 51–61, https://doi.org/10.1016/j.jaut.2017.09.008.
[35] F.F. Wagner, U. Wesmall yi Michel, M.C. Lewis, E.B. Holson, Small molecule inhibitors of zinc-dependent histone deacetylases, Neurotherapeutics 10 (2013) 589–604, https://doi.org/10.1007/s13311-013-0226-1.
[36] A. Platzer, T. Nussbaumer, T. Karonitsch, J.S. Smolen, D. Aletaha, Analysis of gene expression in rheumatoid arthritis and related conditions offers insights into sex-bias, gene biotypes and co-expression patterns, PLoS One 14 (2019) e0219698.
[37] K. Qu, L.C. Zaba, A.T. Satpathy, P.G. Giresi, R. Li, Y. Jin, et al., Chromatin accessibility landscape of cutaneous T cell lymphoma and dynamic response to HDAC inhibitors, Cancer Cell 32 (2017) 27–41, https://doi.org/10.1016/j.ccell.2017.05.008 e4.
[38] S. Hawtree, M. Muthana, A.G. Wilson, The role of histone deacetylases in rheumatoid arthritis fibroblast-like synoviocytes, Biochem. Soc. Trans. 41 (2013) 783–788, https://doi.org/10.1007/s00894-010-0739-z.
[39] R.-J. Lohman, A. Iyer, T.J. Fairlie, A. Cotterell, P. Gupta, R.C. Reid, et al., Differential anti-inflammatory activity of HDAC inhibitors in human macrophages and rat arthritis, J. Pharmacol. Exp. Ther. 356 (2016) 387–396, https://doi.org/10.1124/jpet.115.229328.
[40] A. Dahdah, K. Habir, K.S. Nandakumar, A. Saxena, B. Xu, R. Holmdahl, et al., Germinal center B cells are essential for collagen-induced arthritis, Arthritis Rheum. 70 (2018) 193–203, https://doi.org/10.1002/art.40354.
[41] E.V. Acosta-Rodriguez, L. Rivino, J. Geginat, D. Jarrossay, M. Gattorno, A. Lanzavecchia, et al., Surface phenotype and antigenic specificity of human interleukin 17-producing T helper memory cells, Nat. Immunol. 8 (2007) 639–646, https://doi.org/10.1038/ni1467.
[42] N. Manel, D. Unutmaz, D.R. Littman, The differentiation of human T(H)-17 cells requires transforming growth factor-beta and induction of the nuclear receptor RORgammat, Nat. Immunol. 9 (2008) 641–649, https://doi.org/10.1038/ni.1610.
[43] S.M.J. Paulissen, J.P. van Hamburg, W. Dankers, E. Lubberts, The role and modulation of CCR6+ Th17 cell populations in rheumatoid arthritis, Cytokine 74 (2015) 43–53, https://doi.org/10.1016/j.cyto.2015.02.002.
[44] C. Angiolilli, P.A. Kabala, A.M. Grabiec, I.M. Van Baarsen, B.S. Ferguson, S. García, et al., Histone deacetylase 3 regulates the inflammatory gene expression programme of rheumatoid arthritis fibroblast-like synoviocytes, Ann. Rheum. Dis. 76 (2016) 277–285, https://doi.org/10.1136/ard.2011.150326.
[45] Y. Guo, A.M. Walsh, U. Fearon, M.D. Smith, M.D. Wechalekar, X. Yin, et al., CD40L-Dependent pathway is active at various stages of rheumatoid arthritis disease progression, J. Immunol. 198 (2017) 4490–4501, https://doi.org/10.4049/jimmunol.1601988.